Res2NetFuse: A Fusion Method for Infrared and Visible Images

Xu Song, Xiao-Jun Wu, Hui Li, Jun Sun, Member, IEEE, and Vasile Palade, Senior Member, IEEE

Abstract—This paper presents a novel Res2Net-based fusion framework for infrared and visible images. The proposed fusion model has three parts: an encoder, a fusion layer and a decoder, respectively. The Res2Net-based encoder is used to extract multiscale features of source images, the paper introducing a new training strategy for training a Res2Net-based encoder that uses only a single image. Then, a new fusion strategy is developed based on the attention model. Finally, the fused image is reconstructed by the decoder. The proposed approach is also analyzed in detail. Experiments show that our method achieves state-of-the-art fusion performance in objective and subjective assessment by comparing with the existing methods.

Index Terms—Infrared image, visible image, multi-scale, training strategy, attention model, image fusion.

I. INTRODUCTION

MAGE fusion is an important task in image processing, which aims to integrate salient features of source images into a single image by using a fusion method [1]. Fusion of infrared and visible images is a chalenging task in image fusion. Due to different imaging principles of infrared and visible images, they contain different information about the same scene. Therefore, solving the problem of fusing infrared and visible images is important in many applications.

Many methods have been proposed in the area of image fusion. Generally speaking, the multiscale transform (MST) method is the most common method in the field of image fusion. The main steps of MST-based methods include decomposition, fusion and reconstruction. However, the MST-based methods will loose the effective information of the source image in the process of inverse transform, thus affecting the final fusion results [2].

In recent years, image fusion methods based on representation learning have been widely developed. In sparse representation (SR), Liu et al. [3] obtained global and local saliency maps of the source images based on sparse coefficients for fusion. Liu et al. [4] proposed a general framework of image fusion by combining MST and SR to overcome the inherent defects of the MST- and SR- based fusion methods. In low-rank representation (LRR), Li et al. [5] obtained a better

This work was supported by the National Key Research and Development Program of China (Grant No. 2017YFC1601800), the National Natural Science Foundation of China (61672265, U1836218), the 111 Project of Ministry of Education of China (B12018).

Xu Song, Xiao-Jun Wu(Corresponding author), Hui Li and Jun Sun are with the School of Artificial Intelligence and Computer Science, Jiangnan University, Wuxi 214122, China.(e-mail:xu_song_jnu@163.com; xiao-jun_wu_jnu@163.com; hui_li_jnu@163.com; sunjun_wx@hotmail.com).

Vasile Palade is with the Faculty of Engineering, Environment and Computing at Coventry University, Conventry CV1 5FB, U.K.(e-mail:ab5839@coventry.ac.uk)

performance in both global and local structure by combining LRR and dictionary learning simultaneously.

With the development of deep learning, many image fusion methods based on deep learning were proposed. In 2017, Liu et al. [6] presented a method that can generate the activity level measurement and fusion rule jointly under a convolutional neural network (CNN) model. In 2018, Li et al. [7] used the pretrained VGG-19 [8] to extract the features. Then, they made full use of middle layer features to generate the fused image. In 2019, Li et al. [9] proposed a novel deep learning architecture of image fusion, called DenseFuse. The fusion framework consists of encoding network, a fusion layer and decoding network. But they did not consider multi-scale features in their network. To solve this problem, Song et al. [10] proposed a MSDNet for medical image fusion. They added a multi-scale layer at the end of the encoder of Li's [9] to get multi-scale features and achieved a good fusion effect.

Therefore, from the multi-scale perspective, in this paper we embed the idea of Res2Net [11] into the encoder. Res2Net is a new multi-scale backbone architecture, which will be introduced in SectionII-A. The main contributions of the proposed fusion method are given below:

- (1) Res2Net is used for the fast time in image fusion. We applied Res2Net into our encoder, which extracts muti-scale image features at a more granular level.
- (2) An interesting aspect is that we found that by using only a single natural image we can learn an effective reconstruction model, and the performance of the reconstruction model is comparable with the reconstruction model trained by 80000 images. This has greatly reduced the training time of the proposed model.
- (3) A fusion strategy was developed to use the attention model to produce a weight map for the salient features of the source images.

The structure of the rest of the paper is as follows. In SectionII, we briefly introduce Res2Net and DenseFuse, respectively. In SectionIII, we introduce the the proposed method in detail. In SectionIV, experiment results will be shown, and SectionV is the conclusion of our paper.

II. RELATED WORKS

A. Res2Net

Multi-scale features play an important role in many image processing tasks. In PAMI 2020, Gao et al [11] presented a novel building block for CNN, called Res2Net. The Res2Net module is shown in Fig. 1

In Fig. 1, after the 1×1 convolution, the feature map subsets are obtained by splitting the feature maps evenly, denoted by

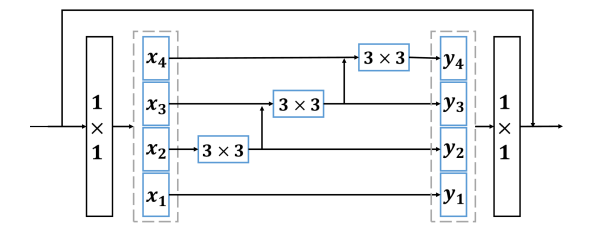


Fig. 1. The graph of Res2Net module.

 x_i , where $i \in \{1, 2, ..., n\}$ and n represents the number of subsets. Except for x_1 , the rest of subsets have a corresponding convolution denoted as $F_i()$. The output of $F_i()$ is marked with y_i . Thus, y_i can be calculated by Eq.1

$$y_i = \begin{cases} x_i & i = 1\\ F_i(x_i) & i = 2\\ F_i(x_i + y_{i-1}) & 2 < i \le n \end{cases}$$
 (1)

As shown in Eq.1, when x_i goes through 3×3 convolutional layer, the output result (y_i) can have a larger receptive field than x_i . Finally, concatenating all splits and passing them through a 1×1 convolution. Therefore, the idea of Res2Net is constructing hierarchical residual-like connections within a residual block. Res2Net extracts multi-scale features at the granularity level and increases the receptive field range for each network layer.

B. DenseFuse

The DenseFuse architecture consists of an encoding network, fusion layer and decoding network. The training network consists of encoder and decoder, and its purpose is to reconstruct the input image. Therefore, training images are not necessarily of the same type as the test images. Hence, the training dataset is easy to get. After the training process, the trained encoder and decoder, respectively, have the ability to extract features and reconstruct the image. Both of them are used in the fusion network. The architecture of DenseFuse is described in Fig.2.

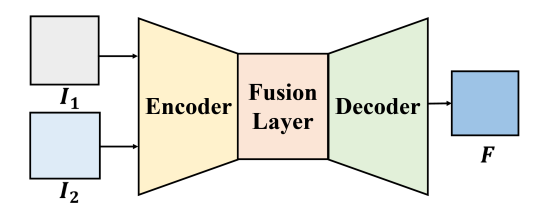


Fig. 2. The DenseFuse framework.

In Fig.2, after encoding, two groups of features are fused in the fusion layer. Finally, the fused image is reconstructed by the decoder.

III. METHODOLOGY

In this section, we will introduce in detail the proposed fusion method for grayscale images. How to process color images will be introduced in SectionIV-D. The three subsections are: the proposed method in III-A; training network (loss function and training strategy) in III-B; fusion layer(strategy) in III-C.

A. The Proposed Method

Inspired by the success of DenseFuse and Res2Net, we use the Res2Net module for the encoder because of its strong ability to extract multi-scale features.

The input images are infrared and visible images, denoted as I_1 and I_2 . We assume the input images are already registered. Our proposed architecture includes the encoder, the fusion layer and the decoder. The architecture of the proposed method is shown in Fig. 3.

As shown in Fig. 3, in the fusion model, the encoder consists of two 3×3 filters and a block of Res2Net. For the Res2Net block, after a 1×1 convolution, all features are split evenly. The operation and the specific formula for the Res2Net block are described in SectionII-A. At the end of the Res2Net block, all splits are concatenated and pass them through a 1×1 convolution. The decoder is constructed by four 3×3 filters. The fusion strategy in the fusion layer will be introduced later.

B. Training

Regardless of color or gray scale images being used, the training network is the same. The training network has just two parts: the encoder and the decoder. The function of the training network is to reconstruct the input image. Therefore, the training network can also be called a reconstruction model. After the training process, we add the fusion layer between the encoder and the decoder. The architecture of the training network is shown in Fig.4. The parameters of the training network are outlined in TableI.

TABLE I THE OUTLINE OF THE TRAINING NETWORK. CONV3 AND CONV1 DENOTE THE CONVOLUTIONAL LAYER WITH 3×3 FILTER AND 1×1 FILTER, RESPECTIVELY. [CONV3] $\times2$ DENOTES TWO IDENTICAL LAYERS.

	Layer	Size	Stride	Input Channel	Output Channel	Activation
Encoder	Conv3	3	1	1	32	ReLU
	Conv3	3	1	32	64	ReLU
	Res2Net Block	-	-	-	-	_
Decoder	Conv3	3	1	64	64	ReLU
	Conv3	3	1	64	32	ReLU
	Conv3	3	1	32	16	ReLU
	Conv3	3	1	16	1	_
Res2Net Block	Conv1	1	1	64	64	ReLU
	-	-	-	-	16	_
	[Conv3]×2	3	1	16	16	ReLU
	[Conv3]×2	3	1	16	16	ReLU
	[Conv3]×2	3	1	16	16	ReLU
	Conv1	1	- 1	64	64	ReLU

Reconstruction Loss. In order to reconstruct the input image, we use the loss function [9] as shown in Eq.2.

$$L = L_{ssim} + L_{nixel} \tag{2}$$

The ${\cal L}_{pixel}$ and the ${\cal L}_{ssim}$ are respectively calculated as:

$$L_{pixel} = \frac{1}{BCHW} ||O - I||_2^2$$
 (3)

$$L_{ssim} = 1 - SSIM(O, I) \tag{4}$$

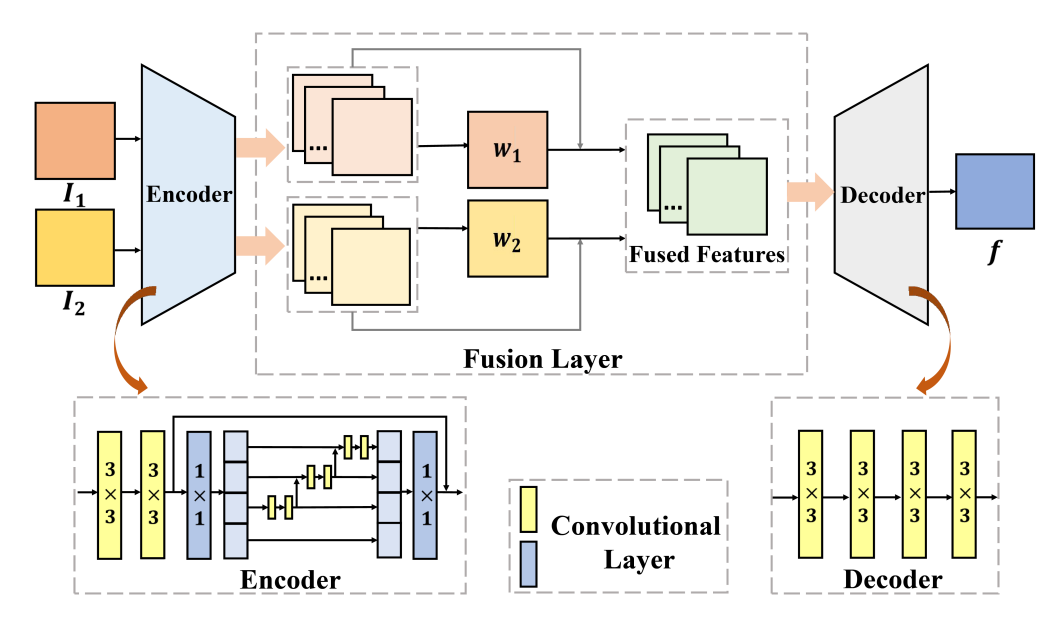


Fig. 3. The architecture of the proposed method for gray scale images.

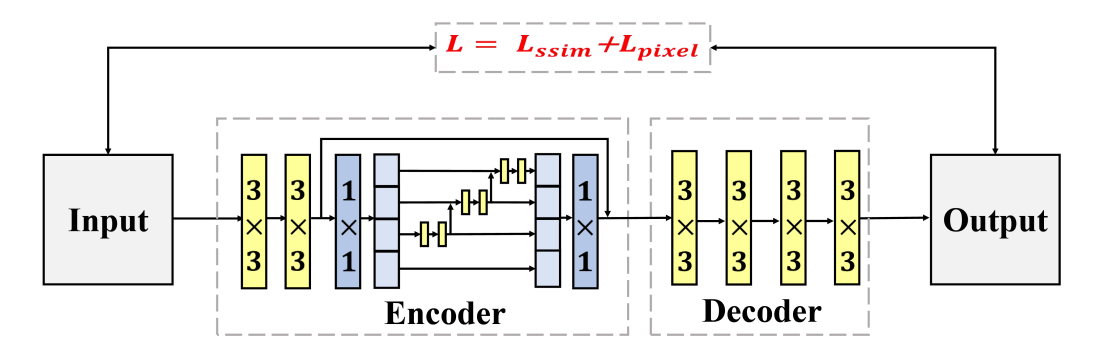


Fig. 4. The reconstruction model.

where O and I are output and input images respectively, B represents the batch size, C is the number of channels of O, H and W are height and width of O. In addition, $SSIM(\cdot)$ denotes the structural similarity [12].

Training Strategy. In an ICCV 2019 paper [13], the authors proved that the internal statistics of patches within a natural image own enough information for learning a powerful generative model. Authors use a single natural image at multiple scales to train a generative model, rather than many samples from a database.

Inspired by [13], at first, we tried a single natural image at different scales to train a reconstruction model. However, experiments showed that the model has the ability to reconstruct the input image, but the details of the output image are slightly blurry.

Therefore, we just tried using a whole natural image to train the reconstruction model 2000 times. Finally, the results show that the reconstruction ability of the model is comparable with DenseFuse [9] and MSDNet [10], which are trained by 80000 images. Moreover, the training time is greatly reduced.

The assessment and the analysis of the training strategy will be dicussed in detail in the IV-B subsection.

Hence, we just randomly choose a natural image (grayscale)

from MS-COCO [14] as being our training sample to train the reconstruction model.

C. The Fusion Layer

The fusion strategy plays an important role in image fusion, and this section will detail our fusion strategy.

Input images have their own distinctive features, therefore, two groups of features will be obtained after encoding. Then, we need two weight maps to fuse them, but the average strategy is too rough. Therefore, as shown in Fig.3, we propose to apply a spatial attention model to the fusion layer.

1)Spatial Attention Based on 1_1 -norm. Inspired by [9], we use an l_1 -norm to process the features extracted by the encoder. Then, we obtain two weight maps, w_1 and w_2 , which are computed by Eq.5

$$w_i(x,y) = \frac{\sum_{j=1}^m ||\phi_i^j(x,y)||_1}{\sum_{i=1}^k \sum_{j=1}^m ||\phi_i^j(x,y)||_1}$$
(5)

where $\phi_i^{1:m}$ are the feature maps extracted by the encoder, m and k, respectively, denote the number of feature maps and input images. In this paper, k=2.

Finally, the enhanced(fused) features denoted as $f^{1:m}$ are calculated by Eq.6.

$$f^{1:m} = \sum_{i=1}^{k} w_i \times \phi_i^{1:m}$$
 (6)

2)Spatial Attention Based on Mean Operation. Firstly, we use mean operation to process the features extracted by the encoder $\phi_i^{1:m}$. Then, we apply the soft-max operation to get the weight maps w_1 and w_2 , as shown in Eq.7.

$$w_i(x,y) = \frac{M(\phi_i^{1:m}(x,y))}{\sum_{i=1}^k M(\phi_i^{1:m}(x,y))}$$
(7)

where $M(\cdot)$ is the mean operation to process the pixel at position (x,y) of each feature map. Then, the fused features $f^{1:m}$ are calculated by Eq.8.

$$f^{1:m} = \sum_{i=1}^{k} w_i \times \phi_i^{1:m}$$
 (8)

After the fusion layer, the final fused features $f^{1:m}$ are fed into the decoder and the fused image is reconstructed accordingly.

IV. EXPERIMENTAL RESULTS

This section firstly introduces the experimental settings and environment. Then, a detailed discussion on the performance of our training network that can be obtained using a single training image is done. The results of the experiments will also be presented, and, finally, we will explain how to process RGB images.

A. Experimental Settings and Environment

In our experiment, there are 20 pairs of test images (infrared and visible images) [9]. Several samples of test images are shown in Fig.5

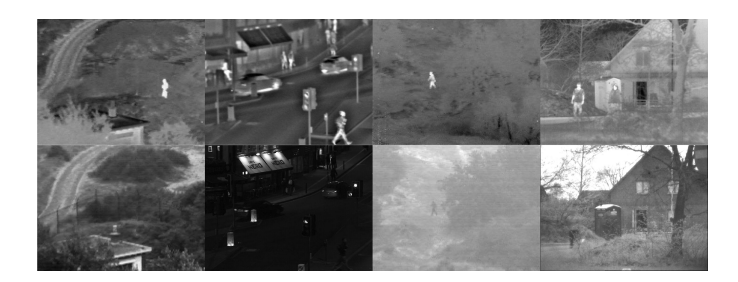


Fig. 5. Four pairs of source images. The first row is infrared images and the second row is visible images.

Comparison methods include the discrete cosine harmonic wavelet transform method(DCHWT) [15], the joint sparse representation-based method(JSR) [16], the fusion method based on saliency detection in sparse domain(JSRSD) [3], DenseFuse [9], FusionGAN [17], and MSDNet [10].

In order to evaluate the fusion results in an objective assessment, we choose eight indices as follows: entropy(EN) [18] that indicates how much information the fusion result contains; mutual information(MI) [19] that measures the amount of information of the source images that the fused image contains;

 Q_{abf} [20] reflects the quality of visual information; the sum of the correlations of differences(SCD) [21] that indicates the amount of transferred information from each of the input images into the fused image; a new no-reference quality assessment for image fusion(MS_SSIM) [22]; FMI_{dct} and FMI_w [23], which calculate the feature mutual information, such as discrete cosine and wavelet features; $SSIM_a$ which is calculated by Eq.9.

$$SSIM_a(f) = (SSIM(f, I_1) + SSIM(f, I_2)) \times 0.5$$
 (9)

where f means the fused image, $SSIM(\cdot)$ denotes the structural similarity operation [12]. The values of $SSIM_a$ measure the structural information of the source images.

In the training phase, the number of iterations is 2000 and the batch size is 1. In addition, the number of training images (grayscale) is 1 and the size of training image is 256×256 .

Our method was implemented with NVIDIA GTX 1050Ti GPU, and Pytorch was utilized as the backend for the network framework.

B. Detailed Discussion of the Training Strategy

Natural images have strong internal data repetition [24]. The analysis of the internal predictive-power was shown to be strong for almost any natural image [25].

Motivated by these observations, we combined the predictive power of internal information and the generalization capabilities of deep-Learning to train our reconstruction model by a single natural image. Therefore, the training strategy consists in that we utilize a natural image to train the reconstruction model 2000 times.

Firstly, we will show the loss graph of our training strategy in Fig.6. As we can see, after 200 iterations, the training model begins to become stable. Then, we display the comparison results to prove the effectiveness of the trained model from the perspective of reconstruction and fusion.

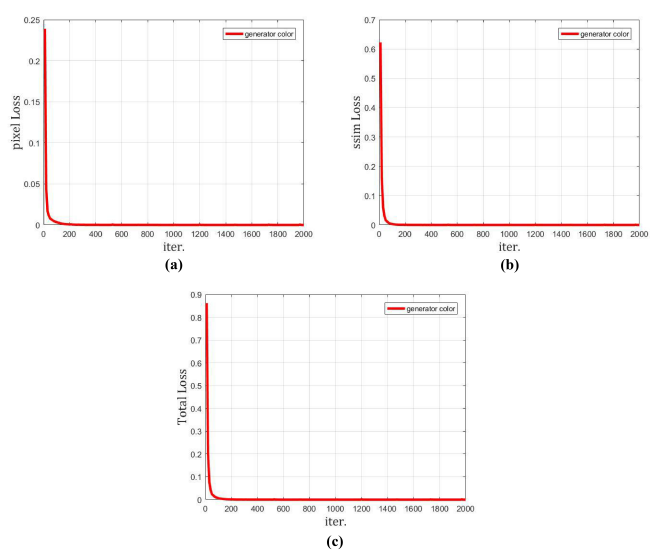


Fig. 6. The graphs of loss. (a) L_{pixel} ; (b) L_{ssim} ; (c)Total loss

•

TABLE II The average values of quality metrics for 20 fused images. l_1 -norm and mean means fusion strategy.

Methods		$SSIM_a$	EN	MI	Q_{abf}	FMI_{dct}	FMI_w	SCD	MS_SSIM
DenseFuse		0.72829	6.66296	13.32592	0.43454	0.41456	0.42525	1.83379	0.92860
MSDNet	l_1 -norm	0.76365	6.40040	12.80079	0.44416	0.37547	0.41741	1.61825	0.83311
	Mean	0.77453	6.28483	12.56966	0.39214	0.39046	0.41116	1.67953	0.87041
Res2NetFuse_80000	l_1 -norm	0.70881	6.83607	13.67214	0.47354	0.37620	0.43160	1.67887	0.84166
	Mean	0.72993	6.77470	13.54940	0.45175	0.40685	0.42417	1.82024	0.91695
Res2NetFuse_1	l_1 -norm	0.72520	6.81785	13.63569	0.48364	0.37552	0.42924	1.69888	0.85384
	Mean	0.74206	6.76675	13.53350	0.46368	0.40262	0.42334	1.83464	0.92129

TABLE III

THE AVERAGE VALUES OF QUALITY METRICS FOR 20 RECONSTRUCTED IMAGES. DenseFuseRecons denotes the reconstruction model of DenseFuse. MSDNetRecons denotes the reconstruction model of MSDNet. Res2NetFuseRecons_1 denotes the reconstruction model of Res2NetFuse trained by an image.

Res2NetFuseRecons_80000 denotes the reconstruction model of Res2NetFuse trained by 80000 images.

Methods	SSIM	PSNR	MSE
DenseFuseRecons	0.99560	43.62612	0.00016
MSDNetRecons	0.99933	52.10881	0.00001
Res2NetFuseRecons_1	0.99560	40.36431	0.00042
Res2NetFuseRecons_80000	0.99888	46.50366	0.00005

1) Reconstruction Comparisons: We compare our reconstruction model with existing reconstruction models which are trained by 80000 images. The reconstruction models for comparison are from DenseFuse, MSDNet and our proposed method which is trained by 80000 images (batch size and epoch are all 4). Then, we randomly choose 20 natural images from MS-COCO in order to do reconstruction experiments. We utilize the structural similarity (SSIM), the peak signal to noise ratio (PSNR) and the mean squared error(MSE), calculated by using Eq.10, in order to evaluate the reconstruction performance.

$$MSE = \frac{1}{W \times H} \sum_{x=1}^{W} \sum_{y=1}^{H} (I(x, y) - R(x, y))^{2}$$
 (10)

where W and H are the width and the height of the image, I is the input image and R is the reconstructed image.

The reconstruction comparison results are shown in TableIII. As shown in TableIII, although Res2NetFuse does not achieve the best metrics values, it still obtains comparable reconstruction ability.

Comparing with Res2NetFuseRecons_80000, the reconstruction model trained by one image achieves acceptable reconstruction performance. This means the internal information of a single image is enough to train our lightweight network. Moreover, with this training strategy, our lightweight network needs much less training time.

2) Fusion Comparisons: In this part, for fusion comparison purposes, we also compare Res2NetFuse_1, trained by an image, with DenseFuse, MSDNet and Res2NetFuse_80000 trained by 80000 images. Among the compared methods, MSDNet is also from a multi-scale perspective. Therefore, when comparing MSDNet and Res2NetFuse, we ensured that

the fusion strategy is the same. The fusion comparison results are shown in TableII.

In TableII, the *red* values mean the best values, the *blue* values mean the second-best values, the *green* values mean the third-best values. We can see that Res2NetFuse_1 has comparable fusion ability with the other methods. In addition, although the MSDNet's reconstruction ability is better than that of Res2NetFuse, the fusion results of Res2NetFuse are better than that of MSDNet under the same fusion strategy. The reason is that the activity level maps of MSDNet are for different scales and, on the other hand, that of Res2NetFuse are for all scales. Therefore, the weight maps generated by the avtivity level maps of Res2NetFuse will be more stable.

Comparing with the Res2NetFuse_80000, we find that the metrics values are similar, which means the fusion performace of Res2NetFuse_1 is acceptable. Therefore, even the Res2Netbased fusion model is trained by a single natural image, it can obtain a good fusion performance.

The above comparisons on the performance of reconstruction and fusion proves that our training strategy is effective. Now we will summarize several reasons why the training strategy is effective:

- 1) The proposed method is a lightweight network, in contrast to the deep networks in other computer vision tasks. In theory, the training process could be done with less training data. And for some deep-learning-based image fusion methods, the deep network is mainly used for reconstruction, which requires less training data than a classification task.
- 2) In fact, natural images have strong internal data repetition and the internal statistics often provides strong predictive-power [24]. Therefore, combining the strong generalization abilities of deep-learning, the lightweight network can be trained by a single natural image.
- 3) Multi-scale feature representations of Res2Net are of great importance to the proposed method, which can make it easier for the decoder to reconstruct the image.

Therefore, through a comprehensive consideration, we choose Res2NetFuse_1 as the final fusion model. The Res2NetFuse mentioned later will be trained by a single natural image.

C. Subjective & Objective Evaluation

Our method is tested for 20 images, and three groups of experimental results are shown in Fig.7–Fig.9.

Through perceptual comparison, the fused results of DCHWT have some noise and salient features are not clear. In

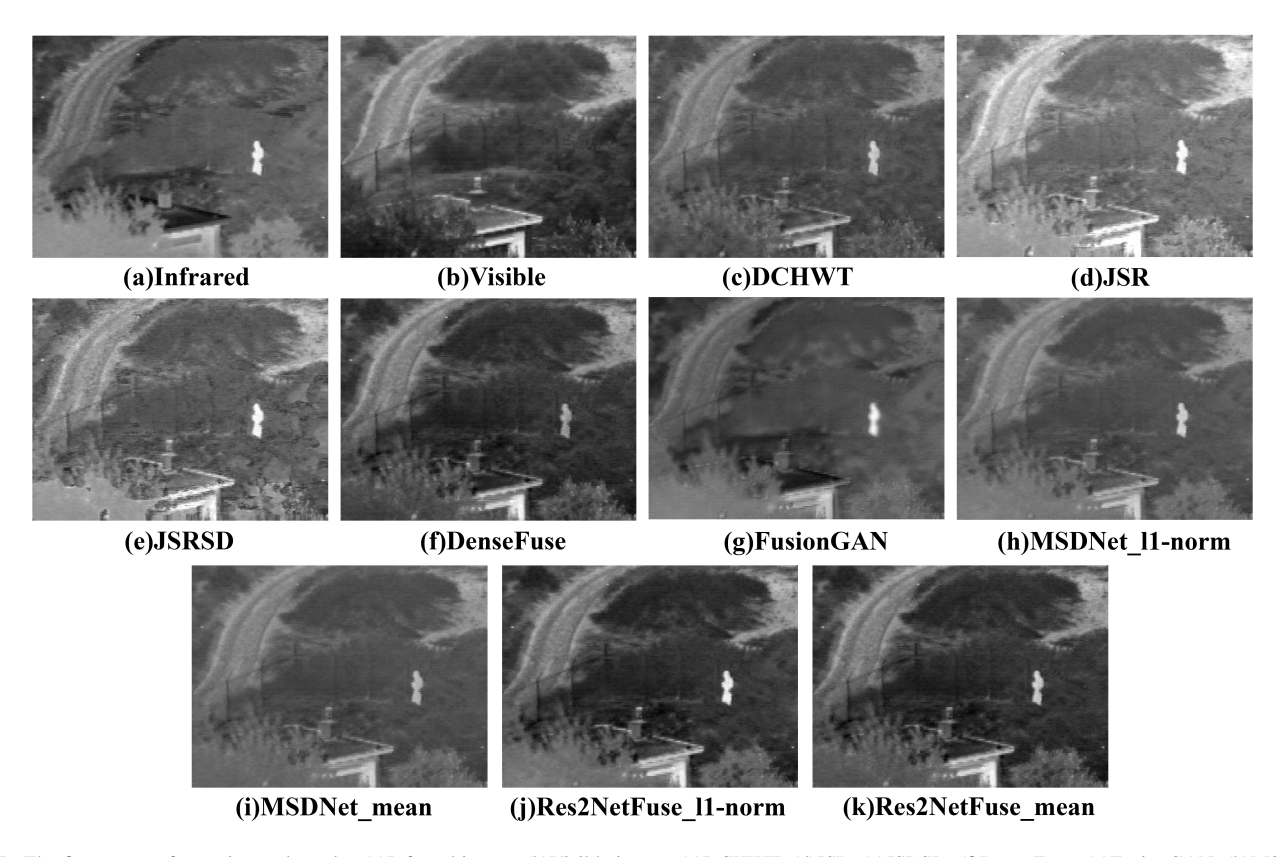


Fig. 7. The first group of experimental results. (a)Infrared image; (b)Visible image; (c)DCHWT; (d)JSR; (e)JSRSD; (f)DenseFuse; (g)FusionGAN; (h)MSDNet with l_1 -norm fusion strategy; (i)MSDNet with mean fusion strategy; (j)Res2NetFuse with l_1 fusion strategy; (k)Res2NetFuse with mean fusion strategy.

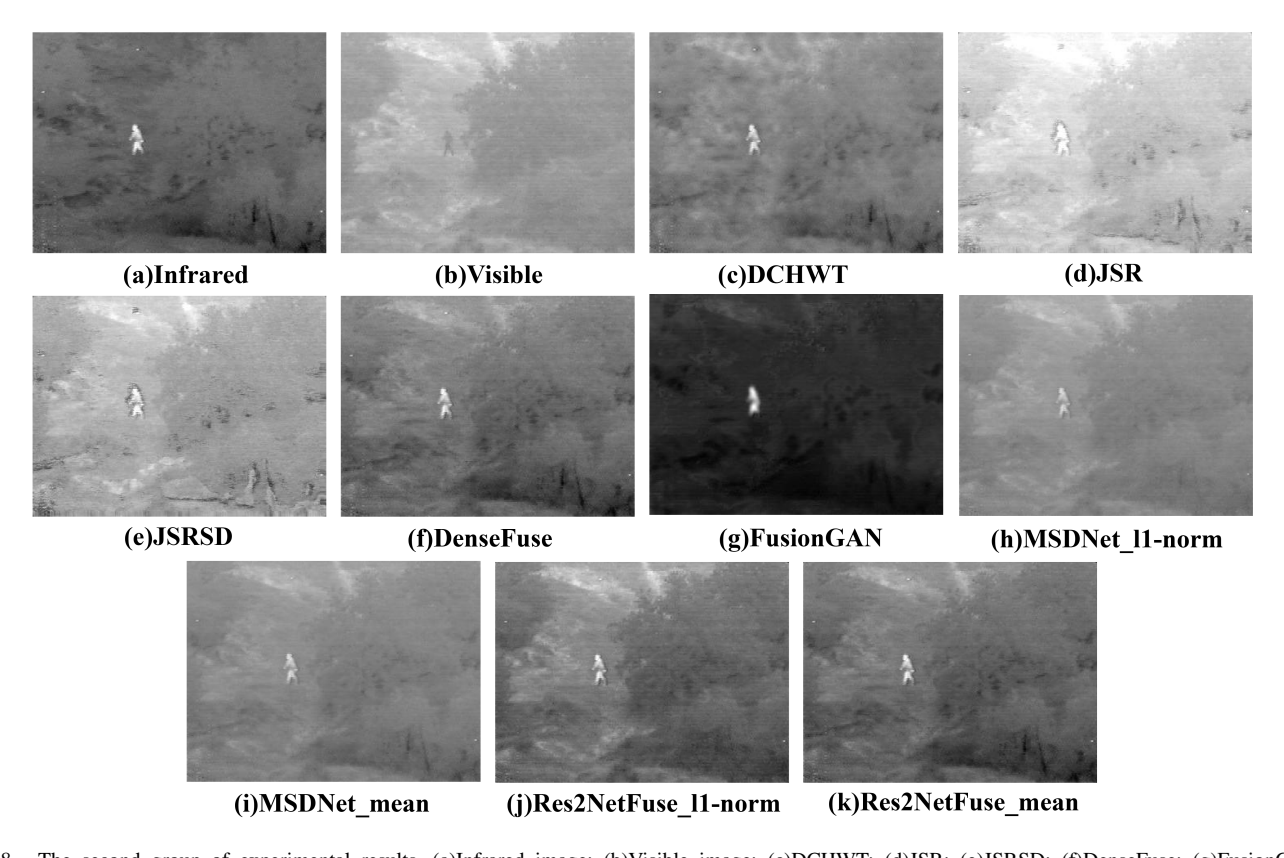


Fig. 8. The second group of experimental results. (a)Infrared image; (b)Visible image; (c)DCHWT; (d)JSR; (e)JSRSD; (f)DenseFuse; (g)FusionGAN; (h)MSDNet with l_1 -norm fusion strategy; (i)MSDNet with mean fusion strategy; (j)Res2NetFuse with l_1 fusion strategy; (k)Res2NetFuse with mean fusion strategy.

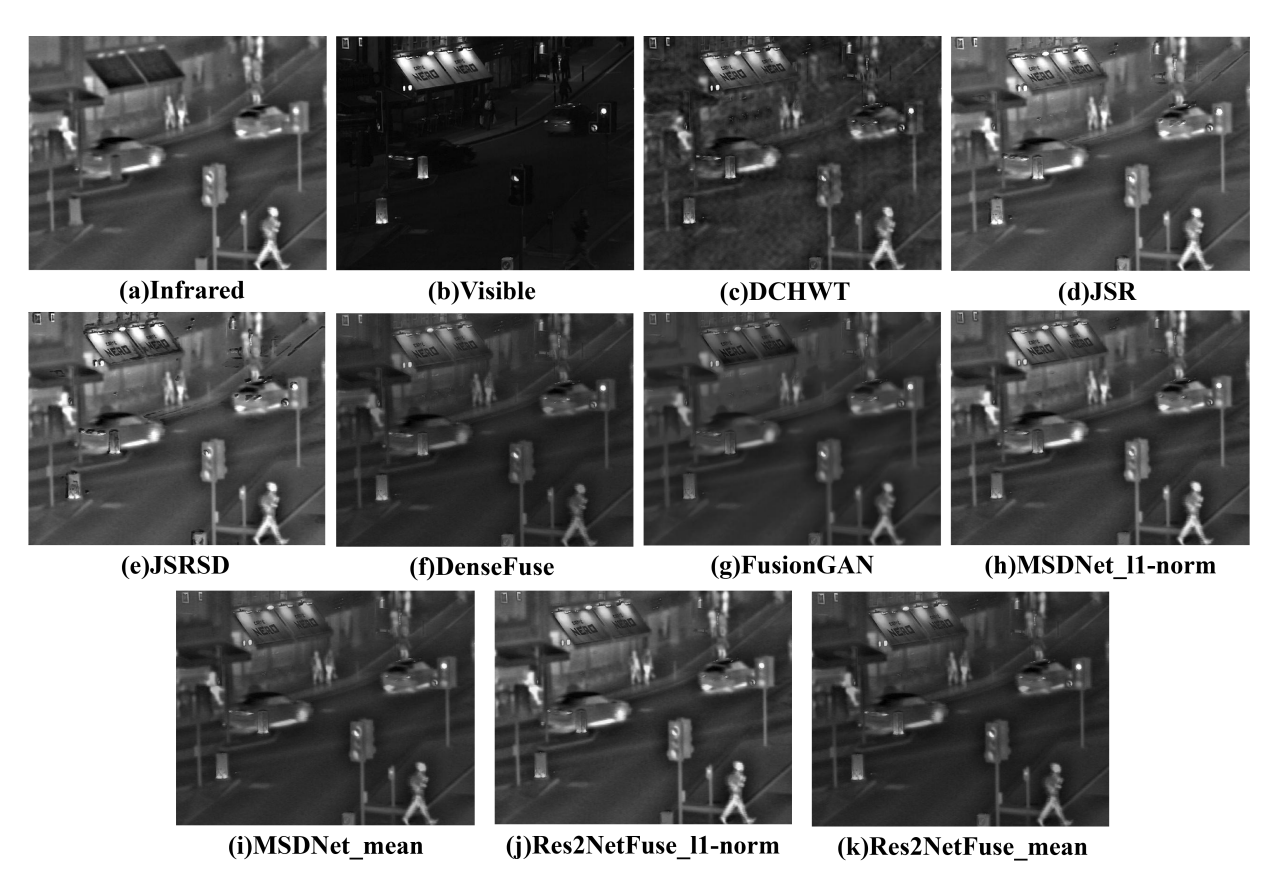


Fig. 9. The third group of experimental results. (a)Infrared image; (b)Visible image; (c)DCHWT; (d)JSR; (e)JSRSD; (f)DenseFuse; (g)FusionGAN; (h)MSDNet with l_1 -norm fusion strategy; (i)MSDNet with mean fusion strategy; (j)Res2NetFuse with l_1 fusion strategy; (k)Res2NetFuse with mean fusion strategy.

addition, the salient features of fused results obtained by JSR and JSRSD are so sharp. Furthermore, as shown in the three figures above, we can find that the results of FusionGAN are not stable, such as shown in Fig.8(g).

On the other hand, the results of Res2NetFuse, MSDNet and DenseFuse are more consistent with human visual standards. But obviously, the results of Res2NetFuse are more stable and have more salient features.

In order to verify objectively the effectiveness of the proposed method, we utilize some indices to evaluate the obtained fused results. The objective evaluation is shown in Table.IV

In Table.IV, the best values are in *red*, the second-best values are marked in *blue* and the third-best values are in *green*. As we can see, Res2NetFuse has some advantages with respect these results of fusion evaluation.

The best values of EN, MI, Q_{abf} , FMI_w and SCD indicate that our method can preserve more visual and salient information of the source images and contain less noise. And second-best values MS_SSIM and FMI_{dct} and third-best value $SSIM_a$ mean that our method preserve more structural information of the source images. In addition, the comparison between Res2NetFuse and MSDNet also indicates that Res2NetFuse could extract more powerful deep features, which are beneficial for image fusion tasks. Therefore, our method is an effective fusion architecture for infrared and visible images' fusion.

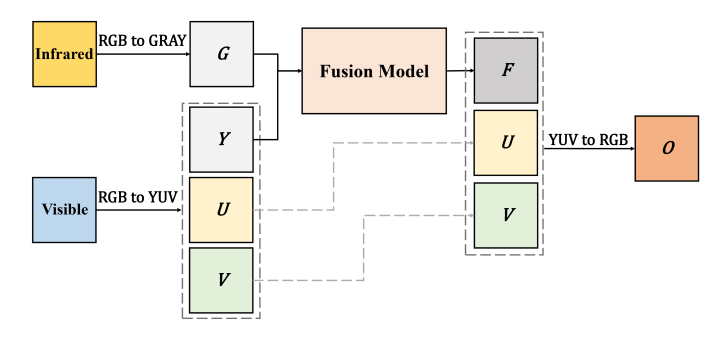


Fig. 10. The fusion framework for color images.

D. Additional Experiments on RGB(Visible) and Infrared Images

Inspired by [26], for color images, we convert the visible image to YUV space and the infrared image to gray sale image. Y channel is the luminance component, in addition, U and V are the chrominance components. We apply our method to fuse the Y channel and the gray scale image. Then, we convert the fused image combined with the U and V channels of visible image to the RGB space. Finally, the fused color image will be obtained. The fusion framework for color images is shown in Fig.10, and the fused color results are shown in Fig.11.

In Fig.11, we can see that the features of fused results are enhanced, which are consistent with human vision perception.

 $\label{table_in_table} \begin{array}{c} \text{TABLE IV} \\ \text{The average values of 20 fused images.} \end{array}$

Methods		$SSIM_a$	EN	MI	Q_{abf}	FMI_{dct}	FMI_w	SCD	MS_SSIM
DCHWT		0.73078	6.53455	13.06910	0.45890	0.38061	0.39700	1.61007	0.84278
JSR		0.60912	6.38043	12.76086	0.36267	0.16738	0.21284	1.75518	0.84735
JSRSD		0.54471	6.66771	13.33541	0.32914	0.14560	0.18697	1.59142	0.76548
DenseFuse		0.72829	6.66296	13.32592	0.43454	0.41456	0.42525	1.83379	0.92860
fusionGAN		0.65207	6.36496	12.72993	0.21853	0.36097	0.36797	1.45818	0.73233
MSDNet	l_1 -norm	0.76365	6.40040	12.80079	0.44416	0.37547	0.41741	1.61825	0.83311
	Mean	0.77453	6.28483	12.56966	0.39214	0.39046	0.41116	1.67953	0.87041
Res2NetFuse	l_1 -norm	0.72520	6.81785	13.63569	0.48364	0.37552	0.42924	1.69888	0.85384
	Mean	0.74206	6.76675	13.53350	0.46368	0.40262	0.42334	1.83464	0.92129



Fig. 11. The fused results for color images. (a)Infrared image; (b)Visible image; (c)Fused results

Therefore, the fusion framework for color images is beneficial for RGB and infrared images' fusion tasks.

V. CONCLUSION

In this paper, we presented a novel architecture for fusion of infrared and visible images based on a multi-scale backbone Res2Net. We found that a single natural image can train the network very well for image fusion. Insights on the success of the proposed method were also presented and analyzed. We proposed to apply an attention model to the fusion strategy, which can generate a more effective weight map to fuse the salient features of source images. The experimental results show that our method outperforms the state-of-the-art methods. In future work, we will apply the proposed training strategy to other tasks of image processing.

REFERENCES

- S. Li, X. Kang, L. Fang, J. Hu, and H. Yin, "Pixel-level image fusion: A survey of the state of the art," *information Fusion*, vol. 33, pp. 100–112, 2017.
- [2] Y. Yang, M. Yang, S. Huang, M. Ding, and J. Sun, "Robust sparse representation combined with adaptive pcnn for multifocus image fusion," *IEEE Access*, vol. 6, pp. 20138–20151, 2018.
- [3] C. Liu, Y. Qi, and W. Ding, "Infrared and visible image fusion method based on saliency detection in sparse domain," *Infrared Physics & Technology*, vol. 83, pp. 94–102, 2017.
- [4] Y. Liu, S. Liu, and Z. Wang, "A general framework for image fusion based on multi-scale transform and sparse representation," *Information fusion*, vol. 24, pp. 147–164, 2015.
- [5] H. Li and X.-J. Wu, "Multi-focus image fusion using dictionary learning and low-rank representation," in *International Conference on Image and Graphics*. Springer, 2017, pp. 675–686.
- [6] Y. Liu, X. Chen, H. Peng, and Z. Wang, "Multi-focus image fusion with a deep convolutional neural network," *Information Fusion*, vol. 36, pp. 191–207, 2017.
- [7] H. Li, X.-J. Wu, and J. Kittler, "Infrared and visible image fusion using a deep learning framework," in 2018 24th International Conference on Pattern Recognition (ICPR). IEEE, 2018, pp. 2705–2710.
- [8] K. Simonyan and A. Zisserman, "Very deep convolutional networks for large-scale image recognition," arXiv preprint arXiv:1409.1556, 2014.
- [9] H. Li and X.-J. Wu, "Densefuse: A fusion approach to infrared and visible images," *IEEE Transactions on Image Processing*, vol. 28, no. 5, pp. 2614–2623, 2018.
- [10] X. Song, X.-J. Wu, and H. Li, "Msdnet for medical image fusion," in International Conference on Image and Graphics. Springer, 2019, pp. 278–288.
- [11] S. Gao, M.-M. Cheng, K. Zhao, X.-Y. Zhang, M.-H. Yang, and P. H. Torr, "Res2net: A new multi-scale backbone architecture," *IEEE transactions on pattern analysis and machine intelligence*, 2019.
- [12] Z. Wang, A. C. Bovik, H. R. Sheikh, and E. P. Simoncelli, "Image quality assessment: from error visibility to structural similarity," *IEEE transactions on image processing*, vol. 13, no. 4, pp. 600–612, 2004.
- [13] T. R. Shaham, T. Dekel, and T. Michaeli, "Singan: Learning a generative model from a single natural image," in *Proceedings of the IEEE International Conference on Computer Vision*, 2019, pp. 4570–4580.
- [14] T.-Y. Lin, M. Maire, S. Belongie, J. Hays, P. Perona, D. Ramanan, P. Dollár, and C. L. Zitnick, "Microsoft coco: Common objects in context," in *European conference on computer vision*. Springer, 2014, pp. 740–755.
- [15] B. S. Kumar, "Multifocus and multispectral image fusion based on pixel significance using discrete cosine harmonic wavelet transform," *Signal*, *Image and Video Processing*, vol. 7, no. 6, pp. 1125–1143, 2013.
- [16] Q. Zhang, Y. Fu, H. Li, and J. Zou, "Dictionary learning method for joint sparse representation-based image fusion," *Optical Engineering*, vol. 52, no. 5, p. 057006, 2013.
- [17] J. Ma, W. Yu, P. Liang, C. Li, and J. Jiang, "Fusiongan: A generative adversarial network for infrared and visible image fusion," *Information Fusion*, vol. 48, pp. 11–26, 2019.

- [18] J. W. Roberts, J. A. van Aardt, and F. B. Ahmed, "Assessment of image fusion procedures using entropy, image quality, and multispectral classification," *Journal of Applied Remote Sensing*, vol. 2, no. 1, p. 023522, 2008.
- [19] M. Hossny, S. Nahavandi, and D. Creighton, "Comments on information measure for performance of image fusion"," *Electronics letters*, vol. 44, no. 18, pp. 1066–1067, 2008.
- [20] C. Xydeas, , and V. Petrovic, "Objective image fusion performance measure," *Electronics letters*, vol. 36, no. 4, pp. 308–309, 2000.
- [21] V. Aslantas and E. Bendes, "A new image quality metric for image fusion: the sum of the correlations of differences," *Aeu-international Journal of electronics and communications*, vol. 69, no. 12, pp. 1890–1896, 2015.
- [22] K. Ma, K. Zeng, and Z. Wang, "Perceptual quality assessment for multi-exposure image fusion," *IEEE Transactions on Image Processing*, vol. 24, no. 11, pp. 3345–3356, 2015.
- [23] M. Haghighat and M. A. Razian, "Fast-fmi: non-reference image fusion metric," in 2014 IEEE 8th International Conference on Application of Information and Communication Technologies (AICT). IEEE, 2014, pp. 1–3.
- [24] A. Shocher, N. Cohen, and M. Irani, ""zero-shot" super-resolution using deep internal learning," in *Proceedings of the IEEE Conference on Computer Vision and Pattern Recognition*, 2018, pp. 3118–3126.
- [25] D. Glasner, S. Bagon, and M. Irani, "Super-resolution from a single image," in 2009 IEEE 12th international conference on computer vision. IEEE, 2009, pp. 349–356.
- [26] H.-Y. Zhang, X.-Q. Luo, X.-J. Wu, and Z.-C. Zhang, "Statistical modeling of multi-modal medical image fusion method using c-chmm and m-pcnn," in 2014 22nd International Conference on Pattern Recognition. IEEE, 2014, pp. 1067–1072.



Xu Song received the B.E. degree in the School of Computer and Information Technology from Liaoning Normal University, China. She is currently pursuing the M.E. degree in the School of Artificial Intelligence and Computer Science from Jiangnan University, China. Her research interests include image fusion and deep learning.



Xiao-Jun Wu received the B.Sc. degree in mathematics from Nanjing Normal University, Nanjing, China, in 1991, and the M.S. degree and Ph.D. degree in pattern recognition and intelligent system from the Nanjing University of Science and Technology, Nanjing, in 1996 and 2002, respectively. From 1996 to 2006, he taught at the School of Electronics and Information, Jiangsu University of Science and Technology, where he was promoted to Professor.

He has been with the School of Information Engineering, Jiangnan University since 2006, where

he is a Professor of Pattern Recognition and Computational Intelligence. He was a Visiting Researcher with the Centre for Vision, Speech, and Signal Processing(CVSSP), University of Surrey, U.K.m from 2003 to 2004. He has published over 300 papers in his fields of research. His current research interests include pattern recognition, computer vision, and computational intelligence. He was a Fellow of the International Institute for Software Technology, United Nations University, from 1999 to 2000. He was a recipient of the Most Outstanding Postgraduate Award from the Nanjing University of Science and Technology.



Hui Li received the B.E. degree in School of Artificial Intelligence and Computer Science from Jiangnan University, China. He is currently a PhD student in the Jiangsu Provincial Engineerinig Laboratory of Pattern Recognition and Computational Intelligence, Jiangnan University. His research interests include image fusion, machine learning and deep learning.



Jun Sun received the Ph.D. degree in control theory and engineering, and the M.Sc. degree in computer science and technology from Jiangnan University, Wuxi, China, in 2009 and 2003, respectively. He is currently a Full Professor with the Department of Computer Science and Technology, Jiangnan University, where he is also the Vice Director of the Jiangsu Provincial Engineering Laboratory of Pattern Recognition and Computational Intelligence. His research interests include computational intelligence, machine learning, bioinformatics, among

others. He has authored or coauthored more than 150 articles in journals, conference proceedings, and several books in the above areas.



Vasile Palade (M'02-SM'04) received the Ph.D. degree from the University of Galati, Romania, in 1999. He was a Lecturer with the Department of Computer Science, University of Oxford, Oxford, U.K., from 2004 to 2013. He is currently a Professor of Artificial Intelligence and Data Science with the Faculty of Engineering, Environment and Computing, Coventry University, UK. His research interests include computational intelligence with applications to image processing, fault diagnosis, and web usage mining, among others. He has published more than

200 articles in journals and conference proceedings, as well as several books.